The British Journal of Radiology, 83 (2010), 206–211

Miliary tuberculosis: a comparison of CT findings in HIV-seropositive and HIV-seronegative patients

[1]J Y KIM, MD, [1]Y J JEONG, [1]K-I KIM, MD, [1]I S LEE, MD, [2]H K PARK, MD, [3]Y D KIM, MD and [3]H SEOK I, MD

Departments of [1]Diagnostic Radiology, [2]Internal Medicine and [3]Thoracic Surgery, Pusan National University Hospital, Pusan National University School of Medicine and Medical Research Institute, Pusan 602-739, Korea

ABSTRACT. The aim of this study was to determine the differences in CT findings of miliary tuberculosis in patients with and without HIV infection. Two radiologists reviewed retrospectively the CT findings of 15 HIV-seropositive and 14 HIV-seronegative patients with miliary tuberculosis. The decisions on the findings were reached by consensus. Statistical analysis was performed using the χ^2 test, Mann–Whitney *U*-test and Fisher's exact test. All of the HIV-seropositive and -seronegative patients had small nodules and micronodules distributed randomly throughout both lungs. HIV-seropositive patients had a higher prevalence of interlobular septal thickening ($p=0.017$), necrotic lymph nodes ($p=0.005$) and extrathoracic involvement ($p=0.040$). The seropositive patients had a lower prevalence of large nodules ($p=0.031$). In conclusion, recognition of the differences in the radiological findings between HIV-seropositive and -seronegative patients may help in the establishment of an earlier diagnosis of immune status in patients with miliary tuberculosis.

Received 7 October 2008
Revised 23 March 2009
Accepted 24 March 2009

DOI: 10.1259/bjr/95169618

Miliary tuberculosis (TB), which results from lymphohaematogenous dissemination of *Mycobacterium tuberculosis*, is a complication of both primary and post-primary TB [1, 2]. This disease results in the formation of small discrete foci of granulomatous tissue, which are uniformly distributed throughout the lung [3].

An increase in TB incidence, including miliary TB, has been associated with infection by human immunodeficiency virus (HIV) [4]. In 2005, the World Health Organization estimated that 12% of HIV deaths globally were caused by TB, and that there were 630 000 new co-infections with TB and HIV [5]. Disseminated TB accounted for 5.4–8.1% of culture-confirmed TB cases, with 10–14% of patients coinfected with HIV having clinically recognisable dissemination [6, 7].

Chest radiography may be helpful in the detection and final diagnosis of miliary TB. The characteristic radiographical findings consist of the presence of fine granular or numerous small nodular opacities measuring 1–3 mm in diameter scattered throughout both lungs [1, 3, 8, 9]. However, the radiograph may appear to be normal in the early stage of disease or in cases with nodules below the threshold of perceptibility; therefore, a diagnosis of miliary TB from chest radiographs can be difficult [10].

Several studies have shown that CT imaging is more sensitive for the detection of parenchymal abnormalities in patients with AIDS who have active intrathoracic disease, and it has been suggested that CT may also be helpful in the differential diagnosis [11–14]. In addition, it has been reported that certain imaging techniques provided by multidetector-row CT are useful for the diagnosis of multiple micronodular infiltrative lung disease [15]. CT findings of miliary TB have been described in previous reports [16–18]; however, only a few studies on miliary TB in patients with HIV, particularly with reference to the CD4 count, have been reported [19, 20]. The radiographic manifestations of HIV-associated pulmonary TB are thought to be dependent upon the level of immunosuppression at the time of overt disease [21–23].

The purpose of this study was to determine the differences in the CT findings of miliary TB for patients with and without HIV infection and to analyse any correlation between the CT features and the level of immunosuppression in patients.

Methods and materials

Our institutional review board approved this retrospective study and waived the requirement for patient informed consent. From January 2003 to January 2008, a computer search was performed to identify all patients with miliary TB and HIV infection who underwent a chest CT examination; the search identified 15 HIV-seropositive patients with miliary TB, of whom 13 were men and two were women (mean age, 44 years; age range, 34–61 years). All 15 seropositive patients were immunocompromised and had positive results from a Western blot or enzyme-linked immunosobent assay (ELISA) for HIV. All 15 HIV-seropositive patients had no additional pathology except miliary TB.

During the same period, we identified a control group of 14 patients with miliary TB. In all of the control patients, an HIV-seronegative status was documented by negative results from a Western blot or ELISA. The control group comprised four men and 10 women (mean

Address correspondence to: Yeon Joo Jeong, Department of Diagnostic Radiology, Pusan National University Hospital, #1–10, Ami-Dong, Seo-Gu, Pusan 602-739, Korea. E-mail: lunar9052@hanmail.net

age, 58 years; age range, 21–89 years). Underlying conditions were identified in 5 of the 14 HIV-seronegative patients: pregnancy ($n=3$) and diabetes mellitus ($n=2$).

The criteria for a diagnosis of miliary TB were the presence of a miliary pattern on a CT image or evidence of multi-organ involvement, along with one or more of the following features: (i) clinical features compatible with TB, including cough for a duration of three weeks or more, fever, weight loss, night sweats, loss of appetite or haemoptysis; (ii) a positive acid-fast bacilli smear or culture; and (iii) histopathological evidence of TB. The diagnosis of miliary TB was made by a demonstration of the presence of *M. tuberculosis* in sputum or bronchial lavage fluid ($n=17$), a transbronchial lung biopsy ($n=5$), an extrathoracic nodal biopsy ($n=4$) or a mediastinal nodal biopsy ($n=1$). The remaining two patients had a diagnosis of miliary TB with classical imaging findings and response to antituberculous medication.

All patients underwent contrast-enhanced helical CT using a four-row multidetector CT scanner (LightSpeed QX/i; GE Medical Systems, Milwaukee, WI). Imaging parameters of the contrast-enhanced CT scans were as follows: 2.5 mm collimation, pitch of 6, reconstruction thickness of 2.5 mm, reconstruction interval of 1.25 mm, 120 kV, and 200–250 mA. Intravenous contrast material (Ultravist; Schering, Berlin, Germany) was used in all 29 patients at a rate of 2.5 ml s^{-1} using a power injector (MCT Plus; Medrad, Pittsburgh, PA); the contrast material was administered through an 18-gauge intravenous catheter located in the antecubital vein.

Two observers (Y.J.J and J.Y.K), who had no knowledge of the HIV status of the patients, reviewed the CT scans. A final decision regarding the findings was determined by consensus. The observers interpreted the CT scans retrospectively in terms of nodules, ground-glass attenuation (GGA), consolidation, peribronchovascular interstitial thickening, interlobular septal thickening and cavities. The findings of fibrocalcified TB, *e.g.* fibrotic bands, bronchiectasis or calcification, were also recorded, as was the presence of lymphadenopathy, pleural effusion, pericardial effusion and extrathoracic involvement of TB. The definition of each CT finding was based on a recently published article [24].

The nodules were assessed for size, distribution and number. Large nodules were defined as having a short-axis diameter of 1 cm or larger, as measured on a CT scan. Nodules smaller than 1 cm in diameter were classified as ''small'' [25]. Nodules smaller than 3 mm in diameter were classified as ''micronodules'' [24]. The distribution of small nodules and micronodules within the secondary pulmonary lobule was classified into ''centrilobular'', ''military'' and ''perilymphatic''. The number of small nodules and micronodules was estimated by counting nodules in two contiguous 4 cm^2 squares on three selected scan levels — the upper (just above the aortic arch), middle (at the level of the bronchus intermedius) and lower (at the level of the lower portion of the left atrium) lung zones.

The extent of GGA was graded as follows: Grade 0 = none; Grade 1 = areas of GGA <25% of the lung parenchyma; Grade 2 = areas of GGA 25–50% of the lung parenchyma; Grade 3 = areas of GGA 50–75% of the lung parenchyma; and Grade 4 = areas of GGA >75% of the lung parenchyma.

Lymph nodes were considered enlarged when they were greater than 10 mm in the short-axis diameter. The presence of a necrotic portion within the lymph nodes was evaluated.

Statistical analyses were performed using commercially available software (SPSS 10.0; SPSS, Chicago, IL). Demographic data (sex and age) of HIV-seropositive and -seronegative patients were evaluated using the χ^2 and Mann–Whitney *U*-tests. Statistical differences among the CT findings of miliary TB for HIV-seropositive and -seronegative patients were analysed by use of the χ^2, Mann–Whitney *U* and Fisher's exact tests. The CT findings of miliary TB in HIV-seropositive patients were compared with the degree of immunosuppression, as indicated by the CD4 T-lymphocyte count. *p*-Values <0.05 were regarded as indicating statistical significance.

Results

There was a statistically significant difference in the sex ratios ($p=0.002$, χ^2 test) between HIV-seropositive and HIV-seronegative patients. Mean ages ($p=0.077$, Mann–Whitney *U*-test) were not significantly different between HIV-seropositive and -seronegative patients.

The CT findings of miliary TB in 15 seropositive and 14 seronegative patients are summarised in Table 1. The most common findings were micronodules and small nodules, which were seen in all 29 patients. Nodules were 1–5 mm in diameter; however, most of the nodules were within the range of 1–3 mm in diameter. All of the small nodules and micronodules had a miliary distribution within the secondary pulmonary lobule (Figures 1–3). The nodules were distributed uniformly throughout the lungs without zonal predominance. The number of small nodules and micronodules in seropositive patients was larger than that in seronegative patients (Table 2). However, there was no statistical significance (Mann–Whitney *U*-test, $p=0.747$).

There was a statistically significant difference in the prevalence of large nodules seen on CT between seropositive and seronegative patients. The seropositive patients had a lower prevalence of large nodules (Table 1; Fisher's exact test; $p=0.031$).

GGA was identified in 14 (93%) of 15 seropositive patients and nine (64%) of 14 seronegative patients. However, there was no statistically significant difference in the presence and extent of GGA between seropositive and seronegative patients ($p=0.722$; χ^2 test; Table 1, Figure 2).

Interlobular septal thickening was identified in all seropositive patients. There was a statistically significant difference in the prevalence of interlobular septal thickening depicted on CT images between seropositive and seronegative patients. ($p=0.017$, Fisher's exact test; Table 1, Figure 3).

None of the HIV-seropositive patients showed a cavity. Cavities were detected in only 2 (14%) of 14 seronegative patients. However, there was no statistically significant difference in the prevalence of cavities seen on CT images between seropositive and seronegative patients (Table 1).

Necrotic lymph nodes were observed in 11 (73%) of 15 seropositive patients and in 3 (21%) of 14 seronegative patients ($p=0.005$; Fisher's exact test; Table 1, Figure 3).

Table 1. Comparison of the CT findings of miliary TB in patients with and without HIV

CT findings	Seropositive patients (%) (n=15)	Seronegative patients (%) (n=14)	p-Value
Micronodules	15 (100)	14 (100)	
Small nodules	15 (100)	14 (100)	
Large nodules	1 (7)	6 (43)	0.031
GGA			0.722
Grade 0	1 (7)	5 (36)	
Grade 1	9 (60)	3 (21)	
Grade 2	2 (13)	3 (21)	
Grade 3	1 (7)	1 (7)	
Grade 4	2 (13)	2 (14)	
Consolidation	0 (0)	2 (14)	0.224
Peribronchovascular interstitial thickening	5 (33)	1 (7)	0.099
Interlobular septal thickening	15 (100)	9 (64)	0.017
Cavity	0 (0)	2 (14)	0.224
Findings of fibrocalcified TB	2 (13)	3 (21)	0.465
Necrotic LN	11 (73)	3 (21)	0.005
Pleural effusion	7 (47)	4 (29)	0.316
Pericardial effusion	5 (33)	1 (7)	0.099
Extrathoracic involvement	10 (67)	4 (29)	0.040

GGA, ground-glass attenuation; TB, tuberculosis; LN, lymph node.

The prevalence of extrathoracic involvement of TB also differed significantly between the seropositive and seronegative patients; extrathoracic involvement affected 10 (67%) of 15 seropositive patients and 4 (29%) of 14 seronegative patients (p=0.040; Fisher's exact test; Table 1, Figure 3). Sites of extrathoracic involvement were most commonly the neck or abdominal lymph nodes (n=10) and spleen (n=5) in the seropositive patients. The site of extrathoracic involvement in all seronegative patients was the spine.

Figure 1. Miliary tuberculosis in a 33-year-old woman not infected with HIV. A lung window of a transverse thin-section CT (1.0 mm section thickness) scan obtained at the level of the left upper lobar bronchus shows uniform-sized small nodules and micronodules randomly distributed throughout both lungs. Also note the subpleural and subfissural micronodules (arrows).

A CD4 T-lymphocyte count was available for 14 seropositive patients. The mean CD4 T-lymphocyte count in these patients was 89 cells μl^{-1} (range, 9–254 cells μl^{-1}). Seven patients had a CD4 count of less than 50 cells μl^{-1} (mean, 29 cells μl^{-1}; range, 9–42 cells μl^{-1}) and seven had a CD4 count of at least 50 cells μl^{-1} (mean, 150 cells μl^{-1}; range, 62–254 cells μl^{-1}).

The CT findings in nine patients with lower levels of immunosuppression (CD4 >50 cells μl^{-1}) were not significantly different from those in eight patients with more profound immunosuppression (CD4 count <50 cells μl^{-1}) (Table 3).

Discussion

A number of investigators have described the CT features of miliary TB, which consist of miliary nodules, GGA and reticular opacity [16–18]. To the best of our knowledge, however, a comparison of the CT features of miliary TB in HIV-seropositive and -seronegative patients has not been reported.

It is well known that unusual or atypical manifestations of pulmonary TB are common in patients with impaired host immunity. The radiographical manifestations of HIV-associated pulmonary TB are believed to be dependent on the level of immunosuppression at the time of overt disease [21–23].

In our study, interlobular septal thickening, the presence of necrotic lymph nodes suggesting TB lymphadenitis, and extrathoracic involvement were more commonly seen in miliary TB patients with HIV infection, whereas large nodules were more commonly seen in miliary TB patients without HIV infection. These results were similar to findings presented in a report by Leung et al [26]. These investigators reported that HIV-seropositive patients with a CD4 T-lymphocyte count of <200 mm^{-3} had a higher prevalence of mediastinal and/

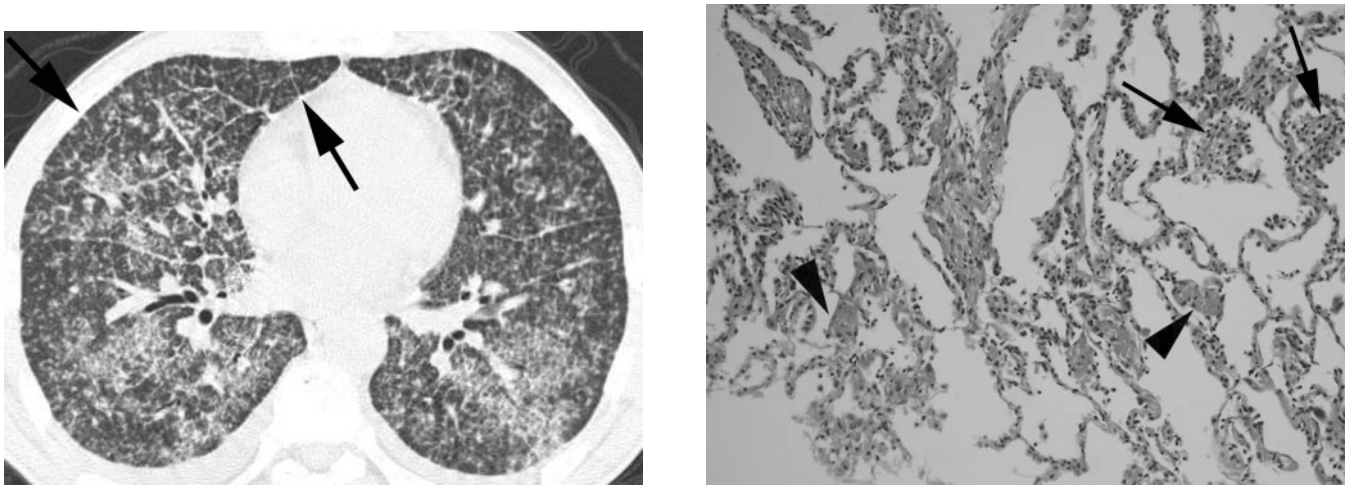

(a) (b)

Figure 2. Miliary tuberculosis presenting as acute respiratory distress syndrome in a 45-year-old man not infected with HIV. (a) A lung window of a transverse thin-section CT (1.0 mm section thickness) scan obtained at the level of the inferior pulmonary vein shows randomly distributed small nodules and micronodules with bilateral extensive ground-glass attenuation in both lungs. Also note the interlobular septal thickening (arrows) and intralobular interstitial thickening in both lungs. (b) A photomicrograph of a pathological specimen (haematoxylin and eosin staining; original magnification $\times 400$) obtained with a transbronchial lung biopsy demonstrates poorly formed granulomas (arrows) in the alveolar wall and diffuse alveolar wall thickening and intra-alveolar fibrin deposition (arrowheads), suggesting an early stage of diffuse alveolar damage.

or hilar lymphadenopathy, a lower prevalence of cavitation and often extrapulmonary involvement when compared with HIV-seropositive patients with a CD4-T lymphocyte count $\geqslant 200$ mm^{-3} [26].

Interlobular septal thickening and GGA are also well-known CT findings of miliary TB. It has been reported that innumerable tiny granulomas scattered throughout the pulmonary interstitium could account for interlobular septal thickening [27], and that areas of GGA may represent small granulomas, resulting in minimal thickening of the septal interstitium, alveolar wall thickening or an oedematous change [16, 18]. In our study,

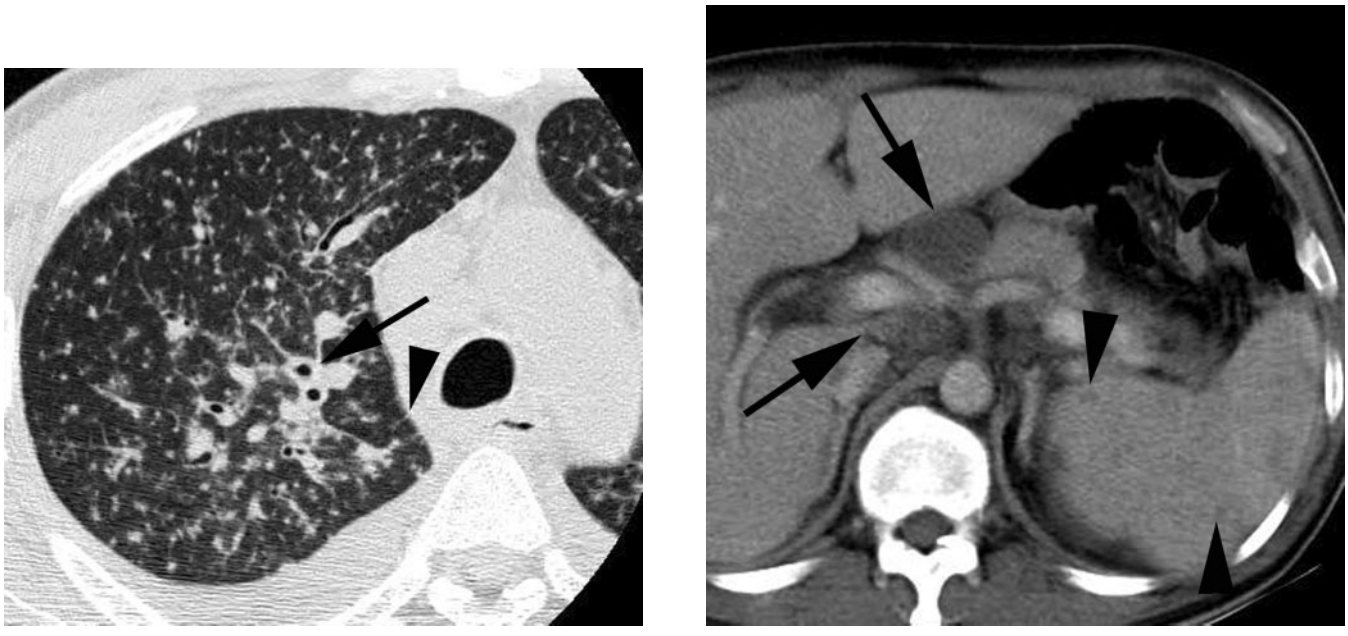

(a) (b)

Figure 3. Miliary tuberculosis with extrathoracic involvement in a 44-year-old man infected with HIV. (a) A lung window of a transverse thin-section CT (1.0 mm section thickness) scan obtained at the level of the aortic arch shows randomly distributed small nodules and micronodules in both lungs. Also note the peribronchovascular interstitial (arrow) and interlobular septal (arrowhead) thickening. (b) A mediastinal window of a transverse contrast-enhanced CT (5.0 mm section thickness) scan at the level of the coeliac axis shows enlarged lymph nodes (arrows) with central low attenuation and peripheral rim enhancement around the coeliac axis, suggesting tuberculous lymphadenitis. Also note the multiple low attenuation nodules (arrowheads) in the spleen.

Table 2. The number of small nodules and micronodules on CT images in patients with and without HIV

Group	Lung zones			Mean
	Upper	Middle	Lower	
Seropositive patients	17.3	20.3	17.3	17.9
Seronegative patients	17.1	17.2	16.2	15.9

Values given in the table are the mean number of small nodules and micronodules in two contiguous 4 cm^2 squares on selected levels.

interlobular septal thickening was identified in all seropositive patients, and there was a statistically significant difference in the prevalence of interlobular septal thickening seen on CT images between seropositive and seronegative patients. In addition, the number of small nodules and micronodules in HIV-seropositive patients was larger than that in HIV-seronegative patients. The number of tiny granulomas scattered throughout the pulmonary interstitium in HIV-seropositive patients may also be larger than that in HIV-seronegative patients. Therefore, interlobular septal thickening was more commonly seen in HIV-seropositive patients in our study. However, there was no statistically significant difference in the presence and extent of GGA between seropositive and seronegative patients. These results suggest that GGA may represent not only small granulomas in the septal interstitium or alveolar wall thickening, but also oedematous or exudative changes of the lung.

Poorly or sharply defined large nodules in the upper lungs are one of the typical and common manifestations of post-primary or reactivation TB [28, 29]. Histologically, the central part of a large nodule consists of caseous material and the periphery of epithelioid histiocytes and multinucleated giant cells and a variable amount of collagen [29]. In our study, large nodules were less commonly seen in miliary TB patients with HIV infection. These results were similar to findings presented in a report by Geng et al [30]. These investigators reported that HIV infection was associated with fewer typical patterned radiographs (consolidation and nodules or cavities in the upper lung zone) and that the altered radiographical appearance of pulmonary TB in HIV was a result of altered immunity.

Greenberg et al [31] have also reported the radiolographical patterns of pulmonary TB according to the degree of immunosuppression. These investigators found that patients with a CD4 T-lymphocyte count of 50–200 mm^{-3} had features of primary TB, including adenopathy, non-cavitary consolidation and pleural effusion, whereas patients with a CD4 T-lymphocyte count below 50 mm^{-3} had diffuse reticular or nodular infiltrates [31]. In our study, we used a CD4 T-lymphocyte count of 50 mm^{-3} as the dividing point to differentiate levels of severe immunosuppression. In contrast to previous studies [26, 31], however, we did not identify any significant difference in the CT manifestations of miliary TB between patients with a CD4 T-lymphocyte count <50 mm^{-3} and those with a count of $\geqslant 50$ mm^{-3}. This discrepancy may reflect a difference in the type of imaging modality used (radiography or CT) or the mean levels of immunosuppression, or may be caused by the small number of patients in this study.

This study has several limitations. Firstly, a relatively small number of patients in our study weakened the value of the statistical results. In addition, the relatively small number of HIV-seropositive patients may not have been sufficient to allow detection of differences in the CT findings for patients with CD4 T-lymphocyte counts of <50 cells μl^{-1} and >50 cells μl^{-1}. Secondly, there was a difference in the age and gender distribution between the HIV-infected and uninfected patients. In our study, sex ratios were significantly different between HIV-seropositive and HIV-seronegative patients. This may be related to the pattern of the sex ratio for AIDS prevalence, pregnancy and unhealthy lifestyle (*e.g.* lack of exercise, sudden excessive weight loss for maintaining thin body habitus) in young female adults. Thirdly, no pathological confirmation was associated with the CT

Table 3. Comparison of the CT findings according to the CD4 level

CT findings	CD4 >50 cells μl^{-1} (%) ($n=7$)	CD4 <50 cells μl^{-1} (%) ($n=7$)	*p*-Value
Micronodules	7 (100)	7 (100)	
Small nodules	7 (100)	7 (100)	
Large nodules	1 (14)	0 (0)	1.000
GGA			0.599
Grade 0	0 (0)	1 (14)	
Grade 1	6 (86)	3 (43)	
Grade 2	0 (0)	2 (29)	
Grade 3	1 (14)	0 (0)	
Grade 4	0 (0)	1 (14)	
Consolidation	0 (0)	0 (0)	
Peribronchovascular interstitial thickening	3 (43)	2 (29)	1.000
Interlobular septal thickening	7 (100)	7 (100)	
Cavity	0 (0)	0 (0)	
Findings of fibrocalcified TB	1 (14)	1 (14)	1.000
Necrotic LN	6 (86)	5 (71)	1.000
Pleural effusion	4 (57)	2 (29)	0.592
Pericardial effusion	3 (43)	2 (29)	1.000
Extrathoracic involvement	6 (86)	4 (57)	0.559

GGA, ground-glass attenuation; LN, lymph node; TB, tuberculosis.

findings for all patients. These findings include interlobular septal thickening, representing innumerable tiny granulomas scattered throughout the pulmonary interstitium, and areas of GGA, representing small granulomas that result in minimal thickening of the septal interstitium, alveolar wall thickening or an oedematous change.

In conclusion, HIV-seropositive patients had a lower prevalence of large nodules and a higher prevalence of interlobular septal thickening, necrotic lymph nodes suggesting TB lymphadenitis and extrathoracic involvement on CT images. Recognition of these differences in the radiological findings between HIV-seropositive and -seronegative patients may assist in an earlier diagnosis of immune status in patients with miliary TB.

References

1. Gelb AF, Leffler C, Brewin A, Mascatello V, Lyons HA. Miliary tuberculosis. Am Rev Respir Dis 1973;108:1327–33.
2. Geppert EF, Leff A. The pathogenesis of pulmonary and miliary tuberculosis. Arch Intern Med 1979;139:1381–3.
3. Sahn SA, Neff TA. Miliary tuberculosis. Am J Med 1974;56:494–505.
4. Sunderam G, McDonald RJ, Maniatis T, Oleske J, Kapila R, Reichman LB. Tuberculosis as a manifestation of the acquired immunodeficiency syndrome (AIDS). JAMA 1986;256:362–6.
5. World Health Organization. Programmes and Projects. Tuberculosis. Address TB/HIV, MDR/XDR-TB and Other Challenges. 2007. Available from: http://www.who.int/tb/challenges/hiv/facts/en/ [Accessed 3 July 2009].
6. Hill AR, Premkumar S, Brustein S, Vaidya K, Powell S, Li PW, et al. Disseminated tuberculosis in the acquired immunodeficiency syndrome era. Am Rev Respir Dis 1991;144:1164–70.
7. Wang JY, Hsueh PR, Wang SK, Jan IS, Lee LN, Liaw YS, et al. Disseminated tuberculosis: a 10-year experience in a medical center. Medicine (Baltimore) 2007;86:39–46.
8. Kwong JS, Carignan S, Kang EY, Muller NL, FitzGerald JM. Miliary tuberculosis. Diagnostic accuracy of chest radiography. Chest 1996;110:339–42.
9. Felson B. Acute miliary diseases of the lung. Radiology 1952;59:32–48.
10. Newell RR, Garneau R. The threshold visibility of pulmonary shadows. Radiology 1951;56:409–15.
11. Kang EY, Staples CA, McGuinness G, Primack SL, Muller NL. Detection and differential diagnosis of pulmonary infections and tumors in patients with AIDS: value of chest radiography versus CT. AJR Am J Roentgenol 1996;166:15–19.
12. Marchiori E, Muller NL, Soares Souza A Jr, Escuissato DL, Gasparetto EL, Franquet T. Pulmonary disease in patients with AIDS: high-resolution CT and pathologic findings. AJR Am J Roentgenol 2005;184:757–64.
13. Knollmann FD, Grunewald T, Neitzert J, Bergmann F, Schedel H, Pohle HD, et al. Thoracic computed tomography of patients infected with the human immunodeficiency virus: relevance for the course of disease. J Thorac Imaging 1999;14:185–93.
14. Kauczor HU, Schnutgen M, Fischer B, Schwickert HC, Hartel S, Schadmand-Fischer S, et al [Pulmonary manifestations in HIV patients: role of thoracic radiography, CT and HRCT]. Rofo 1995;162:282–7.
15. Sakai M, Murayama S, Gibo M, Akamine T, Yoshinaga M, Iraha S, et al. Can maximum intensity projection images with multidetector-row computed tomography help to differentiate between the micronodular distribution of focal and diffuse infiltrative lung diseases? J Comput Assist Tomogr 2005;29:588–91.
16. Oh YW, Kim YH, Lee NJ, Kim JH, Chung KB, Suh WH, et al. High-resolution CT appearance of miliary tuberculosis. J Comput Assist Tomogr 1994;18:862–6.
17. Optican RJ, Ost A, Ravin CE. High-resolution computed tomography in the diagnosis of miliary tuberculosis. Chest 1992;102:941–3.
18. Hong SH, Im JG, Lee JS, Song JW, Lee HJ, Yeon KM. High resolution CT findings of miliary tuberculosis. J Comput Assist Tomogr 1998;22:220–4.
19. Lado Lado FL, Barrio Gomez E, Carballo Arceo E, Cabarcos Ortiz de Barron A. Clinical presentation of tuberculosis and the degree of immunodeficiency in patients with HIV infection. Scand J Infect Dis 1999;31:387–91.
20. Saurborn DP, Fishman JE, Boiselle PM. The imaging spectrum of pulmonary tuberculosis in AIDS. J Thorac Imaging 2002;17:28–33.
21. Murray JF, Mills J. Pulmonary infectious complications of human immunodeficiency virus infection. Part I. Am Rev Respir Dis 1990;141:1356–72.
22. Barnes PF, Bloch AB, Davidson PT, Snider DE Jr. Tuberculosis in patients with human immunodeficiency virus infection. N Engl J Med 1991;324:1644–50.
23. Goodman PC. Pulmonary tuberculosis in patients with acquired immunodeficiency syndrome. J Thorac Imaging 1990;5:38–45.
24. Hansell DM, Bankier AA, MacMahon H, McLoud TC, Muller NL, Remy J. Fleischner Society: glossary of terms for thoracic imaging. Radiology 2008;246:697–722.
25. Webb WR MN, Naidich DP. High-resolution computed tomography findings of lung disease. In: Webb WR MN, Naidich DP, editors. High-resolution CT of the lung. Philadelphia, PA: Lippincott Williams & Wilkins; 2001: 71–192.
26. Leung AN, Brauner MW, Gamsu G, Mlika-Cabanne N, Ben Romdhane H, Carette MF, et al. Pulmonary tuberculosis: comparison of CT findings in HIV-seropositive and HIV-seronegative patients. Radiology 1996;198:687–91.
27. McGuinness G, Naidich DP, Jagirdar J, Leitman B, McCauley DI. High resolution CT findings in miliary lung disease. J Comput Assist Tomogr 1992;16:384–90.
28. Leung AN. Pulmonary tuberculosis: the essentials. Radiology 1999;210:307–22.
29. Jeong YJ, Lee KS. Pulmonary tuberculosis: up-to-date imaging and management. AJR Am J Roentgenol 2008;191:834–44.
30. Geng E, Kreiswirth B, Burzynski J, Schluger NW. Clinical and radiographic correlates of primary and reactivation tuberculosis: a molecular epidemiology study. JAMA 2005;293:2740–5.
31. Greenberg SD, Frager D, Suster B, Walker S, Stavropoulos C, Rothpearl A. Active pulmonary tuberculosis in patients with AIDS: spectrum of radiographic findings (including a normal appearance). Radiology 1994;193:115–19.